Hologram indexing in $LiNbO_3$ with a tunable pulsed laser source

D. A. Woodbury, T. A. Rabson, and F. K. Tittel

The angular and wavelength selectivity characteristics of holograms written with a tunable pulsed dye laser and a cw argon laser were measured. A hologram in a 0.05% weight iron doped crystal was shown to possess ~40% broader bandwidths than a hologram written in a nominally pure crystal of the same thickness. Analyses based on these bandwidths indicate a 430–500-μm effective hologram thickness in a 1-mm thick crystal, which is of the order of the absorption length (380 μm). The implications of these results with respect to optical memories are discussed.

Introduction

There has been considerable interest in the possibility of random access storage of large blocks of information as superimposed thick holograms in photorefractive media such as iron-doped $LiNbO_3$.[1–3] The problem has been studied in considerable detail with cw laser sources being used for both writing and reading of holograms.[4,5] There has also been the use of less stable but more energetic pulsed writing sources, though reading or monitoring of hologram development with well-behaved cw sources is preferred.[6,7]

In this study wavelength and angular selectivity curves were measured and the results compared with theory. Moreover, the feasibility of wavelength indexing was studied directly as part of the wavelength dependence measurements. The work reported in this paper was carried out with a tunable pulsed dye laser source used for both writing and monitoring. The laser pulses were of short duration (7 nsec), moderate power (~20 kW), with nearly negligible exposure per pulse, <1 mJ/cm^2. Single pulse reading provided a sensitive means of detection by taking advantage of the pulse intensity, while hologram erasure was kept to a minimum. The feasibility of angular indexing as described in Ref. 8 has been of particular interest. The possibility of wavelength indexing is mentioned in Refs. 2 and 8, but no data on the wavelength dependence of diffraction efficiency were given. Though thin photographically recorded holograms have been made with a tunable pulsed laser source,[9] there seems to have been no previous attempt to apply such a source to the study of volume holographic storage in $LiNbO_3$:Fe.

Experiment

The tunable pulsed laser source developed for this study is shown in Fig. 1(a). The laser pumping source was a Molectron 400 nitrogen UV laser delivering up to 400-kW peak power in 10-nsec duration pulses. The pulsed dye laser was a two-stage oscillator-amplifier[10] with wavelength descrimination obtained by a intracavity 2-mm, 80% reflective coated etalon and a grating. Pumping of the amplifier was delayed at least one round trip time inside the oscillator in order to allow laser action to develop fully,[11] in the oscillator, before amplification. These precautions tended to minimize the effects of on-axis and off-axis superfluorescence. Several lenses were necessary to couple the oscillator to the amplifier and to collimate the amplifier output. A 10% conversion efficiency was obtained for this type of oscillator-amplifier system.

During writing with the tunable pulsed source, beam reversal was avoided by providing an even number of reflections for each beam as shown in Fig. 1(b) thereby minimizing the dependence on spatial coherence. A delay was included to minimize the path difference to less than the coherence length of the laser source. Direct observation of fringes during these adjustments was facilitated either with a superposition plate as shown in Fig. 1(c) or with a microscope objective. Further optimization of the optical delay during a series of hologram writing experiments suggested a time average coherence length of 3 mm corresponding to a ~10-GHz bandwidth.

The authors are with Rice University, Electrical Engineering Department, Houston, Texas 77001.

Received 26 February 1979.
0003-6935/79/152555-04$00.50/0.

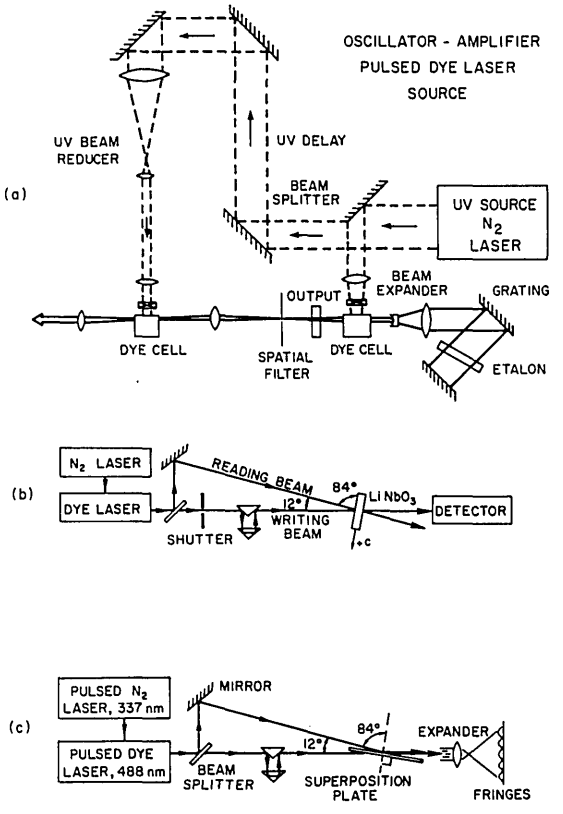

Fig. 1. Experimental arrangement: (a) tunable pulsed laser source with oscillator-amplifier configuration[10,11]; (b) interferometer for hologram writing with this source; (c) optimizing configuration for minimizing path difference.

Holograms written with a cw source were angularly scanned with the tunable pulsed laser source, set at the writing wavelength, and subsequently scanned for wavelength dependence at the optimum angle. Holograms written with the tunable pulsed source were scanned for wavelength dependence at the writing angle and subsequently angularly scanned at the writing wavelength. When the dye laser was operated near the extrema of its tuning range, an additional dispersive grating was used between it and the experiment to remove the excessive superfluorescence. This precaution, along with the pulsed nature of the probe beam, allowed detection of low diffraction efficiencies in these regions. The crystals used in this study were obtained from Crystal Technology and were 1 cm × 1 cm × 1 mm with the c axis along one of the 1-cm directions. The doping levels were 0.05% wt Fe and <0.005% Fe for the doped and nominally pure crystals, respectively.

Results

Figure 2 presents the diffraction efficiency of a hologram that was written with a cw argon laser source at 4880 Å in a nominally pure crystal (×11). A normalized diffraction efficiency may be defined as $\eta/\eta_0 = \eta(\lambda,\theta)/\eta(\lambda_0,\theta_0)$. Here, $\eta_0 = \eta(\lambda_0,\theta_0)$ is the maximum diffraction efficiency measured when the Bragg condition is optimally satisfied, and $\eta = \eta(\lambda,\theta)$ is the diffraction efficiency measured when either λ or θ is varied away from the optimum setting. Thus one measures $\eta/\eta_0 < 1$ as the Bragg condition is less optimally satisfied during these angular and wavelength scans. The wavelength scan of Fig. 2(a) shows a suppression of $\eta/\eta_0 < 0.1$ at 4600 Å. Likewise, the angular scan of Fig. 2(b) shows a suppression of $\eta/\eta_0 < 0.1$ at 0.4° from Bragg incidence.

Figure 3 depicts the characterization for a hologram written with the tunable pulsed source set at 4800 Å in a moderately doped crystal, ×10, with 0.05% wt Fe. The wavelength scan of Fig. 3(a) is confined to the region from 4600 Å to 5000 Å. The angular scan of Fig. 3(b) displays some asymmetry but is also confined to within 0.3–0.5° deviation from Bragg incidence.

The wavelength and angular scans were analyzed on the basis of the complete theory[12] and a simple estimate, both described below. These treatments were used to deduce an effective hologram thickness (EHT) which could then be compared with likely influences such as crystal thickness or absorption length. Routine measurements indicated a transmittance of $T > 70\%$ for crystal ×11 for the wavelengths of interest. This corresponds to an absorption length of $(1/\alpha) > 3$ mm or at least three times the 1-mm crystal thickness. The complete theory yielded an EHT of 660 μm, and estimates indicated an EHT of 750 μm, for the hologram in crystal ×11. These values are at about 70% of the actual crystal thickness. On the other hand, for crystal

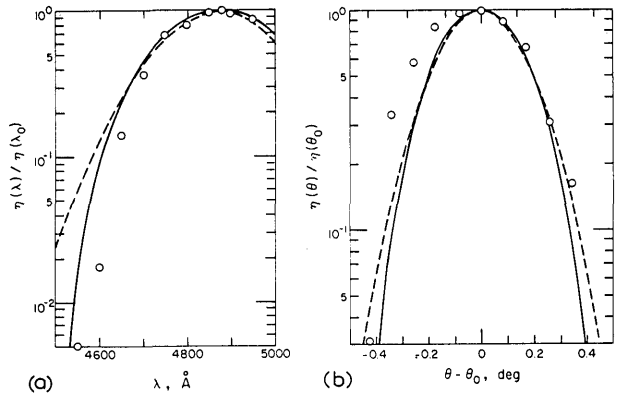

Fig. 2. Simultaneous wavelength and angular scans for a hologram written with cw argon laser in nominally pure crystal ×11 and probed with the tunable pulsed source: (a) normalized diffraction efficiency η/η_0 as a function of wavelength in the vicinity of the writing wavelength; (b) normalized diffraction efficiency η/η_0 as a function of angular deviation from Bragg incidence, both plotted on a log scale. Solid curve is a fit of Eqs. (2)–(5) with $d = 660$ μm for $\eta_0 = 0.05$, and the dashed curve is a fit of Eqs. (6) and (7) with $d = 750$ μm, where the curve fits in (a) have a half power halfwidth of 165 Å and those in (b) have a 0.204° halfwidth.

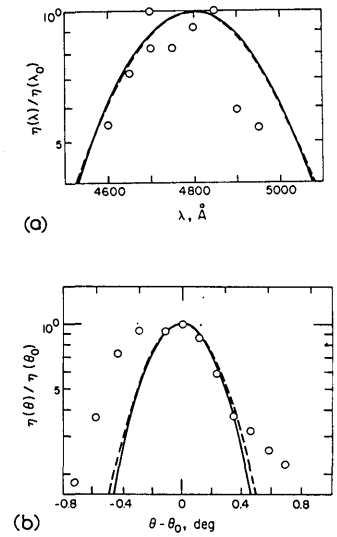

Fig. 3. Simultaneous wavelength and angular scans for a hologram written and as probed with the tunable pulsed dye laser and in moderately doped crystal ×10: (a) wavelength scan; (b) angular scan, both in terms of normalized diffraction efficiency as in Fig. 2. Solid curve is a fit of Eqs. (2)–(5) with $d = 430$ μm for $\eta_0 = 0.5$, and the dashed curve is a fit of Eqs. (6) and (7) with $d = 500$ μm, where the curve fits in (a) have a half power halfwidth of 240 Å, and those in (b) have a 0.30° halfwidth.

×10, $T = (7.4 \pm 0.6)\%$ between 4500 Å and 5000 Å implying a much shorter absorption length of 380 ± 12 μm, which is considerably less than the crystal thickness. The EHT values deduced for the hologram in crystal ×10 were 430 μm and 500 μm for the complete theory and the estimate, respectively. The absorption determines the EHT in this case.

In order to illustrate the feasibility of angular indexing, two wavelength scans are plotted on a linear scale in Fig. 4. Both holograms were written with the same crystal and with the tunable pulsed laser source, but were not superimposed, so that the respective contributions remained distinct. A 30% suppression (or −5 dB) is observed for a separation of less than 200 Å.

Analysis

In the case of a lossless phase grating with the fringes normal to the surface, the diffraction efficiency η is found to be given by[12]

$$\left.\begin{aligned} \eta &= \sin^2(\nu^2 + \xi^2)^{1/2}/(1 + \xi^2/\nu^2) \\ \nu &= \pi \Delta n d/\lambda \cos\theta' \\ \xi &= \vartheta d/2 \cos\theta' \end{aligned}\right\}. \tag{1}$$

Here, Δn is the index of refraction modulation, d the crystal thickness, ϑ a dephasing measure to be described, and θ' the angle of incidence in the medium. When loss is considered a factor of $\exp(-2\alpha d/\cos\theta')$ occurs in η, where α is the absorption coefficient. This modification can be avoided by normalizing the expression to the maximum diffraction efficiency, which is taken as the limiting case of Eq. (1):

$$\eta_0 = \lim_{\xi \to 0} \eta \to \sin^2\nu. \tag{2}$$

This allows the use of the simple form

$$\eta/\eta_0 = (\sin\nu)^{-2} \sin^2(\nu^2 + \xi^2)^{1/2}/(1 + \xi^2/\nu^2). \tag{3}$$

The dephasing measure ϑ in Eq. (1) contains the angular and wavelength dependences. Likewise, ν contains the dependence on refractive index modulation and will be considered constant. For small angular deviations $\Delta\theta'$ in the medium and small wavelength deviations $\Delta\lambda$ measured in free space, one may write

$$\vartheta \cong (K \cos\theta_0')\Delta\theta' - (K^2/4\pi n)\Delta\lambda. \tag{4}$$

Here, θ_0', n, and K are the corrected Bragg angle in the medium, the average refractive index, and grating vector, respectively. The grating vector is related to the fringe spacing Λ by the definition $K = 2\pi/\Lambda$, and the fringe spacing is specified by the Bragg condition $\lambda = 2\Lambda \sin\theta$ for λ and θ measured in a common medium. Equivalently, one has $\Lambda = n\lambda/2 \sin\theta'$ for λ measured in free space and θ' in the hologram recording medium so that one obtains

$$\xi = (\pi d/n\Lambda)\Delta\theta - (\pi d/\cot\theta_0'\Lambda)\Delta\lambda/\lambda. \tag{5}$$

The small angle approximation allows the simple correction of $\Delta\theta'$ to $\Delta\theta/n$ for $\Delta\theta$ measured in free space, but Snell's law must be used to correct θ_0', the angle of incidence inside the medium, so that $\theta_0' = \sin^{-1}[(\sin\theta_0)/n]$, where θ_0 is measured outside the medium.

Equations (2), (3), and (5) may be used to fit the data. Here d is used as an adjustable parameter representing the EHT mentioned above. Both the wavelength and

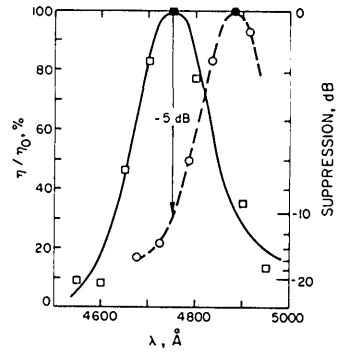

Fig. 4. Normalized diffraction efficiency as a function of wavelength for two holograms written at different wavelengths. The holograms were written in the same crystal at different times.

angular scan data sets for a given hologram may be fit simultaneously with this single adjustable parameter.

As suggested in Ref. 12, estimates of the angular and wavelength half power widths are given by

$$\left.\begin{aligned} 2\Delta\theta_{1/2} &= n\Lambda/d \\ 2\Delta\lambda_{1/2}/\lambda &= \Lambda \cot\theta_0'/b \end{aligned}\right\}. \tag{6}$$

An approximate description of the data may be constructed from Eqs. (6) by using them to specify the half power widths of Gaussian functions. These become

$$\left.\begin{aligned} \eta/\eta_0 &\cong \exp -[(\lambda - \lambda_0)/\Delta\lambda_{1/2}]^2 \ln 2 \\ \eta/\eta_0 &\cong \exp -[(\theta - \theta_0)/\Delta\theta_{1/2}]^2 \ln 2 \end{aligned}\right\} \tag{7}$$

for the wavelength and angular scans, respectively. As before, d is used as the single adjustable parameter in fitting Eqs. (6) and (7) to both data sets and represents an estimate of the EHT. The effect has nodes at finite distances from the origin which are predicted by the complete theory. The absence of these nodes in Eqs. (7) restricts the applicability of this estimate to an interval on the order of the half power width as can be seen from Figs. 2 and 3.

Discussion

The agreement of the experimental results with the two analyses described above is quite good in that no large adjustment of d is necessary. The EHT values deduced by both described analyses are approximately equal to the smaller of either the crystal thickness or the hologram attenuation length. These results are also in reasonable agreement with a calculation for a hologram exponentially attenuated with thickness.[13] The slight variation found may be ascribed to disturbance of the hologram writing process, which would tend to broaden the observed selectivity.

Although the feasibility of angular indexing is well known,[8] wavelength indexing should be retained as a possible alternative or complimentary technique. The wavelength bandwidths are narrower than calculated from the observed angular bandwidths in conjunction with either the complete theory or the estimate. The wavelength scans shown in Fig. 4 indicate that several holograms would be accessible with two or three laser dyes used in the tunable source.

In this study, holograms were written with a tunable pulsed dye laser and with a cw argon laser. The dye laser was used for wavelength and angular scans of holograms. A hologram in a 0.05% wt iron doped crystal was shown to possess bandwidths that were ~40% broader than for a hologram written in a nominally pure crystal of the same thickness. The bandwidths of the holograms were analyzed, and an associated effective hologram thickness was deduced. This thickness was found to be of the order of either the absorption length in the crystal or the crystal thickness, depending on which length was smaller.

This work was supported by the National Science Foundation and the U.S. Army Ballistic Missile Defence Advanced Technology Center.

References

1. D. von der Linde and A. M. Glass, Appl. Phys. 8, 85 (1975).
2. W. J. Burke, D. L. Staebler, W. Phillips, and G. A. Alphonse, Opt. Eng. 17, 308 (1978).
3. A. M. Glass, Opt. Eng. 17, 470 (1978).
4. D. L. Staebler, W. J. Burke, W. Phillips, and J. J. Amodei, Appl. Phys. Lett. 26, 182 (1975).
5. R. Orlowski, E. Kratzig, and H. Kurz, Opt. Commun. 20, 171 (1977).
6. O. F. Schirmer and D. von der Linde, Appl. Phys. Lett. 33, 35 (1978).
7. I. B. Barkan, S. I, Marennikov, and M. V. Entin, Phys. Status Solidi A: 45, K17 (1978).
8. W. J. Burke and Ping Sheng, J. Appl. Phys. 48, 681 (1977).
9. Yu. I. Ostrovski and L. V. Tanin, Sov. Phys., Tech. Phys. 20, 1118 (1975).
10. R. Wallenstein and T. W. Hansch, Opt. Commun. 14, 353 (1975).
11. R. Wallenstein, Opt. Acta 23, 887 (1976).
12. H. Kogelnik, Bell Syst. Tech. J. 48, 2909 (1969).
13. N. Uchida, J. Opt. Soc. Am. 63, 280 (1973).